# POLITECNICO DI TORINO
# UNIVERSITÉ DE PARIS


## Master's Double Degree in Nanotechnologies for ICTs and Quantum Devices

Master's Degree Thesis

# Trapping and manipulating dipolar excitons in two-dimensional lattices of GaAs bilayer


Supervisors

Dr. Camille LAGOIN

Dr. François DUBIN

Prof. Carlo RICCIARDI

Prof. Maria Luisa DELLA ROCCA

Candidate

Marco BACILIERI



June 2020

# Acknowledgements

I would first acknowledge the team Superfluix of INSP for giving the possibility to work with for my internship. The covered topics of the research activity on the quantum physics of new and interesting behavior of exotic phase of matter helped me in expand my acquired knowledge in the wide semiconductor-based devices application.

I would like to thank my thesis advisor Dr. Dubin François of the Institut des NanoSciences de Paris at Sorbonne Université. He consistently allowed this paper to be my own work, but steered me in the right the direction whenever he thought I needed it.

I would also like to acknowledge Dr. Lagoin Camille of the Institut des NanoSciences de Paris at Sorbonne Université as the second reader of this thesis, and I am gratefully indebted to her for her very valuable comments on this thesis. Without her passionate participation and input, the writing could not have been successfully conducted.

Finally, I must express my very profound gratitude to my parents, to my sister and to all my friends for providing me with unfailing support and continuous encouragement throughout my years of study and through the process of researching and writing this thesis. This accomplishment would not have been possible without them. Thank you.

Bacilieri Marco

*"Ετσι, δϵν γνωριζω"*<br>
*"I know that I do not know"*<br>
*Socrates,*<br>
*Athens, 470 a.C. - Athens, 399 a.C.*

# Table of Contents

# List of Figures

# Chapter 1

# Introduction

## 1.1 Exotic states of quantum matter

Two-dimensional heterostructures based on semiconductor quantum wells provide a concrete tool to study neutral electron-hole pairs, quasi-particles called excitons. The bosonic behaviour of the quasi-particles offers the possibility to study non conventional physics and the nature of the bound states open perspectives such as the exploration of exotic phases like super-solidity or suppressed Bose condensation even at zero Kelvin temperature. Originally introduced in 1970's they have been used to explore collective phenomena in semiconductors because they offer a rather unique system to observe two-dimensional superfluidity in the limit of very strong particle interactions.
These bound states offer the possibility to probe exotic quantum phases of collective states, namely gases at thermal equilibrium, reporting signatures of quantum coherence and superfluidity. These gasses don't undergo conventional Bose-Einstein condensation at finite temperatures. The crossover between normal and quasi-condensate phases is observed by the emergence of spatial coherence which is correlated to the quasi-particles' photoluminescence.

## 1.2 Bose-Einstein condensation

The seminar work on this topic was done in this article [1], which represented the starting point for all the successive work as in article [2] and recently in the work [3]. The Bose-Einstein condensate (BEC) is a state of matter in which separate atoms or subatomic particles cooled to near absolute zero, coalesce into a single quantum mechanical entity—that is described by a wave function—on a near-macroscopic scale as shown in Fig. 1.1. According to the Pauli exclusion principle fermions tend to avoid each other, for which reason each electron in a group occupies a separate quantum state marked by different quantum numbers, such as the electron's energy, angular momentum and spin. In contrast, an unlimited number of bosons can have the same energy state and share a single quantum state therefore being marked by equal quantum numbers. BECs are related to two remarkable low-temperature phenomena: superfluidity and superconductivity.

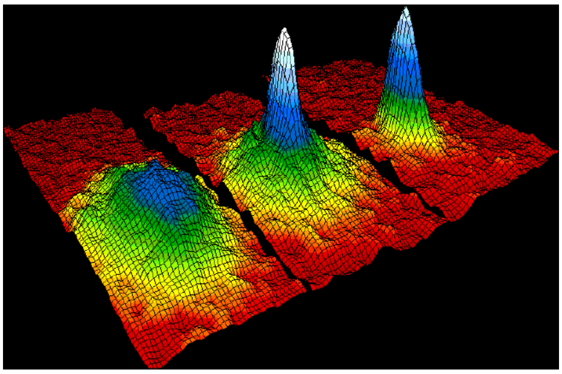

**Figure 1.1:** Velocity-distribution data (3 views) for a gas of rubidium atoms, confirming the discovery of a new phase of matter, the Bose–Einstein condensate. Left: just before the appearance of a Bose–Einstein condensate. Center: just after the appearance of the condensate. Right: after further evaporation, leaving a sample of nearly pure condensate. Source: [1]. From Cornell (1996).

## 1.3 Bose-Hubbard model [4]

The physics of the system is captured by the Bose-Hubbard model, which describes an interacting boson gas in a lattice potential. The hamiltonian in second quantized form reads:

$$H = -J \sum_{<i,j>} \hat{a}_i^\dagger \hat{a}_j + \sum_i \varepsilon_i \hat{n}_i + \frac{1}{2} U \sum_i \hat{n}_i \Big( \hat{n}_i - 1 \Big) \tag{1.1}$$

The first term describe the hopping behaviour between two nearest neighbour through the operators of creation $\hat{a}_i^\dagger$ on sites $i$ and annihilation $\hat{a}_j$ on site $j$. The second term represents the chemical and external potential present in each site. The operator $\hat{n}_i = \hat{a}_i^\dagger \hat{a}_i$ the atomic number operator counting the number of atoms on the $i$ lattice site. The third term represents the on-site interaction between the particles on site $i$. In our application of the Bose-Hubbard model for our studies the $U$ represents the dipolar interaction between the excitons and $J$ depends upon the mass of the particles and the lattice potential: from the evaluation of the overlap between the modulus squared of the wavefunctions in different sites.

### Quantum phases

The balance between the terms in the Hamiltonian describing the system defines two interesting quantum phases:

- **Mott insulator (J=0)**: The system is frozen, for each lattice site the number of particles is constant. In every lattice site the occupied state is the minimum energy state, only one band is filled. The system behaves like an insulator. The state is energetically protected. An energetic high cost to have different number of particles for sites is present. No global phase coherence is observed.

- **Superfluid (J>0)**: Above a critical value for the $J$ for which the minimum of the energy is the state in which the number of particles for lattice site is no more defined, a phase coherence is defined and it arises along the structure beyond the thermal De Broglie wavelength.

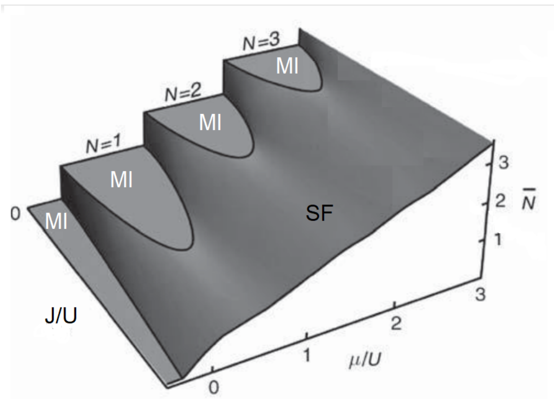


**Figure 1.2:** Bose-Hubbard phase diagram as function of the chemical potential and the coupling. For J=0 the ladder of well defined number of particles of the Mott insulating states with increasing number of particles per unit site is observed. If the hopping it's not suppressed, the system could move from the Mott phase (MI) to the superfluid phase (SF) with the lost of the definition of exact number of particles per unit site. Source: [5]

## 1.3.1 Surperfluid transition to Mott insulator

Non-conventional physics can be explored through quantum phase transitions. To illustrate this idea, we consider an atomic gas of bosons at low enough temperatures that a Bose-Einstein condensate is formed. The condensate is a super-fluid (Fig. 1.3-a), and it is described by a wavefunction that exhibits long-range phase coherence.

An intriguing situation appears when the condensate is subjected to an adjustable lattice potential. In such lattice the bosons could move from one lattice site to the next only by tunnel coupling.
If the lattice potential is turned on smoothly, the system remains in the super-fluid phase. In this regime a delocalized wavefunction minimizes the dominant kinetic energy, and therefore also minimizes the total energy of the many- body system. In the opposite limit, when the lattice potential isn't turned on smoothly, the total energy is minimized when each lattice site is filled with the same number of atoms. In the state with a fixed atom number per site phase coherence is lost. The state of localized particles is the Mott insulating state (Fig. 1.3-b).
The physics of the above-described system is captured by the Bose-Hubbard model, which describes an interacting boson gas in a lattice potential. The competition between hopping and on-site interaction in the hamiltonian is fundamental to understand quantum phase transitions and inherently different from normal phase transitions, which are usually driven by the competition between inner energy and entropy.

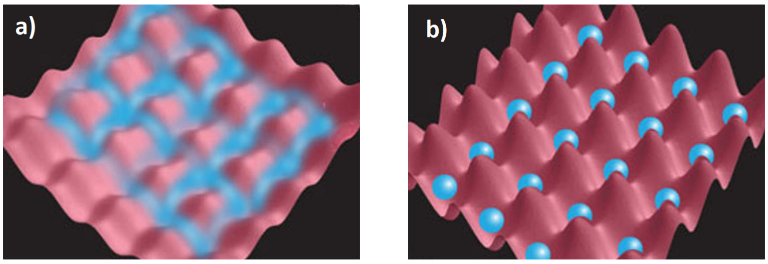


**Figure 1.3:** A prominent example of a quantum phase transition is the change from the super-fluid phase (a) to the Mott insulator phase (b) in a system consisting of bosonic particles with repulsive interactions hopping through a lattice potential.

## 1.4 The state of the art

The state of the art of the devices is the starting point of this internship with the aim of obtain better results. The samples that will be investigates belong to two different group of devices: the singular circular trap designs and the two-dimensional square lattices. For the circular design the aim will be to overcome the limits given by the simplicity of the initial state-of-the-art design [6], by means of designing more complex structures. The study of advanced square lattices will involve the aim to solve the issues related to the non-conventional physics that we want to unveil such as the previously described phase transitions, starting from the work on [7].

# Chapter 2

# Two dimensional dipolar exciton gas

Excitons are quasi-particle created in semiconductors when an electron is promoted from the valence band to the conduction band. The Coulomb interaction between the conduction electron and the valence hole then leads to a bound state, the excitons. In bulk materials excitons are described like hydrogenoid-like systems: their energy levels and wavefunction recall the ones of the hydrogen atom.
In reduced dimensionality structures the behaviour is modified i.e. due to their confinement along one direction. The lifetime of excitons depends on the overlap of the wave-function of the electron and hole which controls the rate of electron/hole recombination. Being made of two fermions, excitons have a predicted bosonic behaviour at densities such that their fermionic characteristic is disguised.

## 2.1 Semiconductor quantum wells devices

### 2.1.1 Direct and indirect excitons

In two dimensional systems the confining environment can be either made of wide single quantum well or double quantum wells, which are artificial semiconductor systems made of alternating higher and lower bandgap materials as shown in Fig.2.1(a-b). In such environments excitons can be classified into direct excitons and indirect excitons. Direct excitons are the result of the excitation of an electron and the successive bonding with the hole within a single quantum well.
Instead indirect excitons can be created either in the wide single quantum well or in a double quantum well structure. To obtain indirect excitons in single quantum well the aim is to get electron and hole pushed apart toward opposite interfaces and therefore an external applied electric field perpendicular to the plane of the of

the single quantum well is required. In a double quantum well structure, in which the single well obtained by alternating high bandgap material with low bandgap material is repeated twice as shown in Fig.2.1, electron and hole must sit in two different wells in order to define indirect exciton quasi-particle. In order to have electron and hole in the different quantum wells after excitation process occurred, the tunneling through the barrier must occurs for one of the two components of exciton, this can be obtained by means of a perpendicular applied electric field as shown in Fig.2.1(c). The tunneling event of a particle through the barrier allow the particle to reach its minimum of the energy. Therefore both in single quantum well and double quantum wells indirect excitons are indeed characterized by the spatial separation of their components.

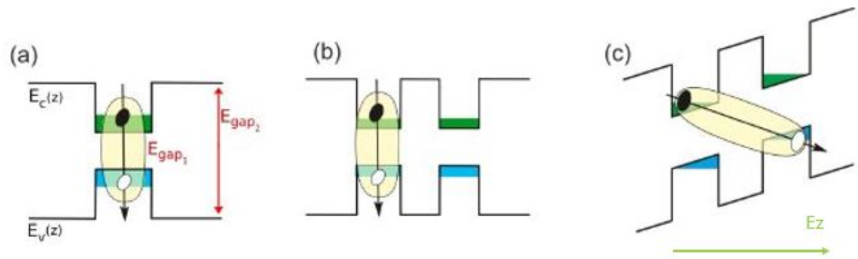


**Figure 2.1:** Energy band diagrams. a) Simple quantum well, with an exciton depicted on it. b) Double quantum well. c) Double quantum wells subjected to a uniform electric field, with an indirect exciton. The Dipolar moments are represented by a wick, electrons by black discs and holes by white discs. In green and blue the probabilities of presence. Source: [6]

### 2.1.2 Excitons lifetime in 2D systems

In GaAs quantum wells unbiased excitons have a short radiative lifetime around 100 *ps* which limits the maximum obtainable value for their density. This lifetime, of the order of the thermalization time, is smaller in 2D than in bulk materials. The study of indirect excitons at thermal equilibrium is achievable due to the fact that the separation between the components of the quasi-particle increases the exciton radiative lifetime. An increase by orders of magnitude of the lifetime is achieved as result of the reduction of the overlap of the electron and hole wavefunctions for electrically polarized wide single quantum well and for electrically polarized double quantum well.

For electrically polarized single quantum well the lifetime is increased up to tens of nanoseconds by means of an external electric field. In the electrically polarized double quantum well heterostructure the overlap of the wavefunctions of electron and hole is reduced such that when biased the lifetime can reach up to hundreds of nanoseconds. The previously mentioned applied electrical field perpendicular to the quantum well plane can be translated by the means of a field effect device with an applied bias voltage. Such electrically polarized excitons are referred as dipolar excitons. The dipolar characteristic derives from the fact that exciton are made of spatially separated opposite charged components, electron with negative unit charge $-e$ and hole with positive unit charge $+e$.

### 2.1.3 Optical injection methods

The pump method allows to reach high temporal resolution in spectroscopic measurements, opening the doors to new experiments describing the dynamics of ultrafast processes. Optical means produce excitons through resonant excitation at the direct exciton energy of the double quantum well, or through non-resonant excitation at the energy above the bandgap of the high bandgap material barrier layers.
For a non-resonant excitation free electron hole pairs with high energy are injected throughout the sample (see Fig. 2.2-a). The energy relaxation of electrons and holes possibly leads to their capture in each of the two QWs so that indirect excitons are formed. Nevertheless this approach is problematic because electrons and holes can be captured in many other places than in the QWs. The electrostatic environment is then poorly controlled. By contrast for a resonant excitation electrons and holes are directly injected in the QWs.
For an excitation resonant with the direct exciton absorption (Fig.2.2(b) in red) injects direct excitons in the lowest energy states of the direct excitons band, directly in the DQW. Tunnelling and relaxation of the carriers towards the minimum energy states then leads to indirect excitons which initially have a large in-plane momentum ($\mathbf{k}$). The gray panel (bottom left of Fig.2.2(b)) shows the fine structure of indirect excitons in GaAs, with energetically separated bright and dark states.

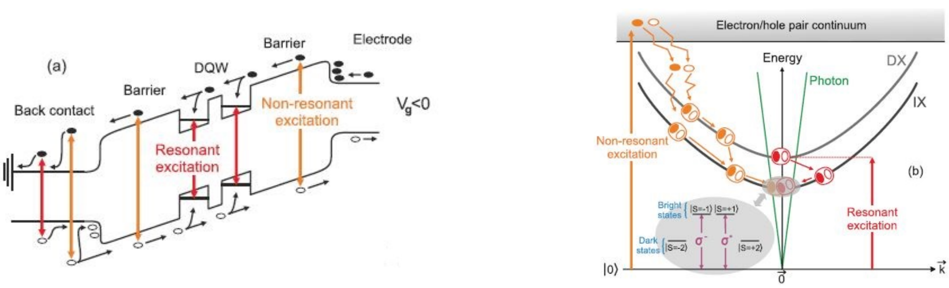


**Figure 2.2:** a) Band diagram of a field-effect device, in the direction perpendicular to the DQW. b) Energy bands for direct excitons (DX) and indirect excitons (IX) in the plane of the quantum wells. Source: [6]

## 2.2 The simple trap idea

### 2.2.1 The dipolar nature of indirect excitons

#### Dipole-dipole interaction

The dominant interaction between indirect excitons is the dipole-dipole interaction. In the frame of the simplest model the strong repulsive dipole-dipole interaction that reduces the indirect excitons density is written in Eq. 2.1 in which $r$ is the distance between excitons, $a$ the exciton diameter and $\kappa = \mu_0 c/2\pi$:

$$u(r) = \frac{2e^2}{\kappa}\left(\frac{1}{r} - \frac{1}{\sqrt{a^2+r^2}}\right) \tag{2.1}$$

The dipole-dipole repulsive energy defined in Eq. 2.2 will stabilize the excitons against the formation of heavier molecules, the energy of this interaction depends upon $n_x$, the density of excitons and $u(\mathbf{r})$, the electrostatic interaction between two indirect excitons:

$$U_{dd} = \int n_x u(\mathbf{r}) d\mathbf{r} \propto n_x \tag{2.2}$$

The repulsive energy will therefore diffuse the indirect excitons across the double quantum well plane reducing their density $n_x$ so a trapping action is required in order to limit this effect.

#### Dipole-field interaction

The high dipolar characteristic of the indirect excitons make them high electric field seeker due to the fact they gain energy from the dipole-field interaction, minimizing their potential energy in the high field regions. In our study we take the axis reference such that the perpendicular direction with respect to the plane of the double quantum well is defined to be the $z$ axis.
The dipole moment of indirect excitons is $\vec{d_x} = ez_0\hat{z}$ with $z_0$ being the distance between the centers of the two quantum wells. The confinement energy written in Eq. 2.3 can be written as function of the the in-plane directions of the double quantum well plane and the perpendicular direction: $\mathbf{r} = (\vec{r}_{//}, z)$. The dipole-field interaction energy is defined through the perpendicular component of the electric field, $\vec{E_z}(\vec{r}_{//}, z)$:

$$U_{df}(\vec{r}_{//}, z) = -\vec{d_x} \cdot \vec{E_z}(\vec{r}_{//}, z) \tag{2.3}$$

### 2.2.2 The circular trap design

#### Engineering of the trap

By using the high value dipole of indirect excitons it's possible to trap them under an inhomogeneus electric field. The confinement is obtained with circular trap design (see top and side view of Fig. 2.3, source [8]). It's possible to conclude that indirect excitons will stay in the region under the gate contact if sufficient voltage is applied between the top contact and the ground electrode. In order to engineer the electric field modulation in the DQW plane the two top contacts are patterned at the sample surface by means of electron beam lithography.
If the the electric field under the green electrode is higher than the electric field under the brown electrode as shown in the Fig. 2.3 then the exciton are confined under the circular green electrode (see top view) which is thus called the trap electrode. The perpendicular component of the electric field $E_z$, is proportional to the potential gradient along z. At the boundary between the trap and the brown electrode which is called the guard electrode, the excitons feel an energy barrier due to the brutal reduction of $E_z$. The indirect excitons experience a trapping dipolar force Eq. 2.4, just near the boundaries, given by the relationship:

$$\vec{F}(\vec{r}_{//}, z) = d_x \frac{\partial E_z}{\partial r_{//}} \vec{r}_{//} \tag{2.4}$$

In the circular trapping geometry if the radius of the trap is bigger than the height of the device then the excitons will feel perfectly reflecting boundary conditions at the edges. In the boundary regions due to the gradient of potential in the radial direction, the radial component of the field can be appreciable.

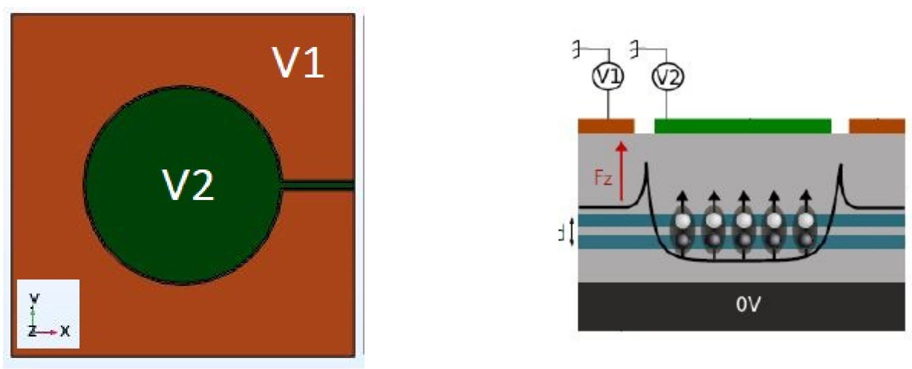


**Figure 2.3:** Top view in the left hand side figure and side view in the right hand side figure. The sample consist of a GaAs substrate of thickness $l$ embeding a DQW layer deposited at a distance $z$ from the bottom of the sample which is used as the ground electrode.

### 2.2.3 Limitations of the trapping

Such trapping method impose though a limitation on the density and on the effective lifetime i.e. the trapping energy should be bigger than the repulsion so minimum required applied electric field is requested. An applied electric field though will translate into a component of it in the plane of the double quantum well.
The presence of a component of the electric field in the plane of the DQW, namely the in-plane component, acting on the constituent of excitons pulling apart them in opposite directions being of charges of opposite sign is a poisonous unwanted effect. The result of the action of the in-plane electric field is the ionization of excitons which correspond to the creation of unbounded carriers decreasing in the lifetime of excitons.

#### Excitons and free carriers poisoning [9], [10]

The simulated two electrodes design suffers of the limitation given by the in-plane component of electric field. High value of this characteristic will lead to presence and accumulation of free carriers therefore imposing a limit on the quality of the two dimensional gas of excitons that is obtainable. This result can be understood as a consequence of the considerably weaker screening of the Coulomb interaction in 2D compared with 3D.

## 2.3 The confining and ionizing fields

The non negligible magnitude of the in-plane electric field, $E_r$, with respect to the perpendicular component, $E_z$, can pull apart the electrons and holes that constitute the excitons therefore ionizing them so the aim is to have it as low as possible. The maximal critical value for the in-plane electric field is reached when $|E_r| \approx \varepsilon_x/(ea_x)$ with $\varepsilon_x$ the dipolar exciton binding energy and $a_x$ the in-plane radius.The relative behaviour of the two components of the electric field is shown in Fig. 2.4.

### 2.3.1 The position of the quantum well plane

In order to avoid this limit the position of the DQW plane is investigated. The normal position of the DQW, $z/l$ ( see Fig. 3.1) is used as parameter for the graph of Fig. 2.4(a) to study the radial component and the z component of the field, this indicate the roadmap for the design of the height of the quantum wells plane.

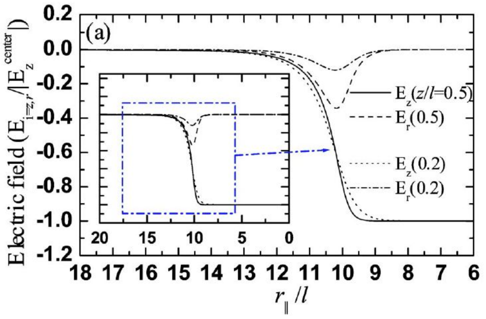


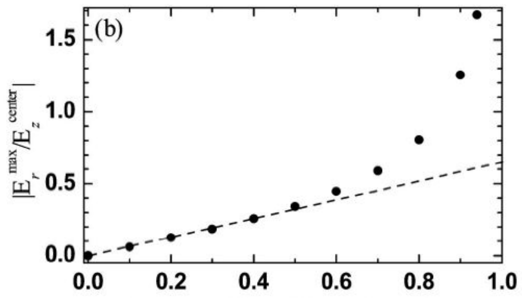


**Figure 2.4:** a) The ratio of the in-plane component of the electric field and the perpendicular component is shown in the plane of the double quantum well, with two possible values of the normal position of the DQW. In the figure it's possible to observe that the perpendicular component of the field is almost unchanged by the different value of the normal position while the in-plane component changes reducing its well peak value for lower normal position. b) The ratio of the maximal value of the radial component of the electric field, to the vertical component of the field at the trap center, for various vertical position z/l values circles (x axis). Source: [11]

The ratio of the in-plane electric field and the perpendicular component shows a linear dependence is found when $z/l < 1/2$ as shown in Fig. 2.4(b):

$$\frac{|E_r^{max}|}{|E_z^{center}|} \approx \beta \frac{z}{l} \tag{2.5}$$

With the parameter $\beta = 0.625$. In conclusion the minimization of $z/l < 0.25$ allows to reduce the $E_r/E_z$ ratio. This minimization would then correspond to a maximum value for excitonic density in the order of $n_x > 10^{10} cm^{-2}$. To describe how $n_x$ changes over time the rate equation is used in Eq. 2.6.

$$\frac{\partial n_x}{\partial t} = -\frac{n_x}{\tau_{trap}} \tag{2.6}$$

As the excitonic density increases the effective lifetime in the trap decreases due to the fact that an higher number of excitons will be closer to the boundaries. The reduction of the ratio of the in-plane component of the field and the perpendicular component correspond in the sample design to move the double quantum well plane closer to the ground away from the surface with the wanted result of increasing the lifetime pf excitons.

## 2.4 Conclusion

The study of indirect excitons and their dipolar nature forms a solid basis for the successive work on the design of circular traps and eventually of lattices. The built knowledge on how the external electric field forms the basics of the understanding of our devices properties. Furthermore the study of the ratio between the in-plane electric field and the perpendicular electric field as function of the geometrical characteristics of the device allowed us to obtain some results on how the geometry itself should be designed in the growth direction of the device.

### 2.4.1 Sample requirements

The degree of quality of the obtained results depends among many requirements. In order to have a good sample a good design need to be defined alongside a good fabrication process. The sample requirements can be enveloped in the following list:

- **Not too much ionization**:
  In the environment of the devices in which the quasi-particles exist, they're characterized by the energy that keep the state bound and their lifetime. Quasi-particles cannot no longer exist if they undergo ionization, namely the separation of he constituent of the bound state creating free-carriers, electrons and holes;

- **Absence of free carrier due to low electrostatic potential disorder**:
  If free carriers, unbound components of the quasi-particles are present, they can undergo interactions with the excitons. Exciton-free carrier collisions due to the Coulomb interaction proved to be stronger by a factor of eight than exciton-exciton collisions. A strong condition on the unwanted presence of free carriers is set because the action of the free carriers reduces the lifetime of the bound states therefore limiting the maximum achievable density for the quasi-particles in the sample;

- **High confinement energy**:
  Due to high value for the dipole energy that characterize indirect excitons, the confinement energy in order to be effective should be greater otherwise the confinement loses its effectiveness.

# Chapter 3

# Circular trap designs

In this chapter, we emphasise box-like trapping potentials for dipolar excitons. At first, we introduce a basic trap architecture made of two electrodes: a central disk imprinting the region of the trap, which is biased stronger than an outer electrode defining the electrostatic potential outside of the trap. We show that such a simple design is efficient, but nevertheless limited by the amplitude of the in-plane electric-field at the boundary between the two electrodes and in the plane of the double GaAs quantum wells. This in-plane electric-field component is damageable, since it tends to ionise dipolar excitons in the vicinity of the trap boundaries. In practice such ionisation leads to an accumulation of free carriers (electron or hole) in the trap.
We then discuss a more advanced design that allows one to partially circumvent this limitation. This more advanced architecture was developed during this internship. It relies on 3 electrodes to better smooth the potential difference between the inside and the outside of the trap. Thus, we show that we essentially reduce the in-plane electric field component in the plane of the quantum wells by around two-fold. At the same time, the depth of the trapping potential is not reduced.

## 3.1 Comsol Multiphysics® simulation tools

To get the results is necessary to use the tools that Comsol Multiphysics®. The program is a graphic software used to design 3D systems and performs finite element method calculation.

### The Finite Element Method

The finite element method is a numerical analysis technique to obtain solutions to the differential equations that describe a wide variety of physical problems. The underlying premise of the method states that a complicated domain can be sub-divided into a series of smaller regions in which the differential equations are approximately solved. By assembling the set of equations for each region, the behavior over the entire problem domain is determined. The process of subdividing a domain into a finite number of elements is referred to as discretization.

In the frame of this work the Electrostatic is the main tool that will be used. Since the study doesn't involve any time dependent evolution, the study will be done in the frame of the Stationary tool. The geometry of the device is built starting from the 3D tools that are available.

### 3.1.1 Geometry and materials

When all the parameters have been uniquely defined in a table, the simulation procedure then requires to construct the Geometry of the wanted device. First, the three dimensional components like the ground electrode and the substrate in which the double quantum well plane is highlighted by dividing the substrate in two different colored layers (green and light green) as shown in the side view of Fig. 3.1. Second, the two dimensional components are then built at the surface of the sample as seen in the top view of Fig. 3.1.

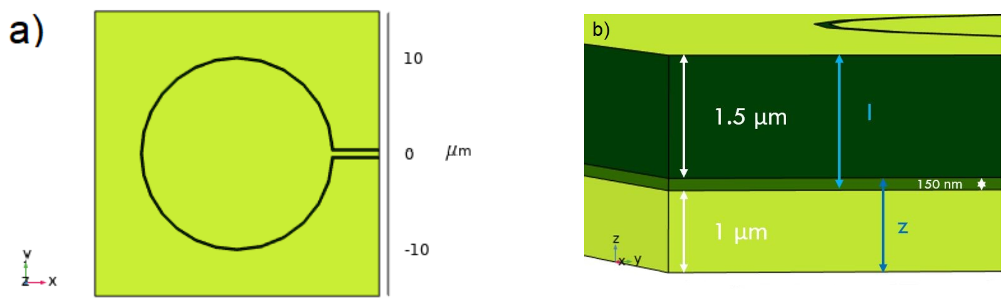


**Figure 3.1:** Insight on the simplest circular design on the top (a) and side (b) views, the top electrodes are separated by a 200 nm region

Ground is the yellow box on the bottom in the side view. The design of the top contacts belong to the last set of components that is designed during this stage of the simulation process and it is indeed here where most of the difficulties and constraints arise whenever the complexity grows. The successive step is to define the materials of the geometric entities previously defined.
Gold has been used in the simulations for the ground and the top contacts. For our purpose of simulations the relative permittivity of gold was set to the value 1. GaAs (refractive index $n = 3.95$) was used as material for the substrate.

**Electrostatic**

Through the Electrostatic tools to define the regions of the top contacts where the voltages and the ground will be applied. Therefore defining the trapping and guarding, the former region with an higher voltage applied with respect to the latter as shown in Fig. 2.3. The electrostatic potential $\phi(\mathbf{r})$ in the system in the absence of excitons was calculated numerically using COMSOL Multiphysics 5.5 software package. The potential was calculated by solving the Laplace equation, defined as Eq. 3.1 in the volume of the box. At the electrode surfaces the boundary condition of constant potential was imposed, e.g., at the ground plane (bottom surface) we have zero potential.

$$\nabla^2\phi(\mathbf{r}) = 0 \tag{3.1}$$

### 3.1.2 Mesh

The Mesh definition is the key for the Finite Element Method used by the Comsol program to run the simulations as shown in Fig. 3.2. In the figure it's shown the finest mesh, this will allow to get the best results for the simulations.

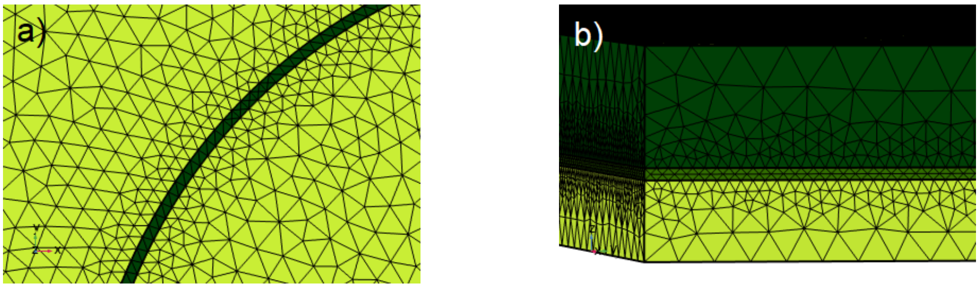


**Figure 3.2:** Mesh representation for the top view (a) and side view (b) for the circular design. The smallest element of the mesh corresponds to the separation between the top contacts is 200 nm

### 3.1.3 Results

The last step to simulate the designed system will be to use the tool Study and get the results for the electric field components and the potential in the double quantum well plane. In Fig. 3.4 the results for the components of the electric field in the circular design are presented.
The perpendicular component of the electric field $E_z$ is shown in two orthogonal cuts along the DQW plane to demonstrate the symmetry of the field deriving from

the symmetry properties of the circular design. The perpendicular component of the electric field defines the box shape of the trapping region. The in-plane components of the field, $E_y$ and $E_x$ show the limitation of this design. In this geometry it's possible to write the dipole-field interaction, which general formula is Eq. 2.3, in terms of the potential difference $\Delta\phi_0$:

$$U_{df}(\vec{r}_{//}=0,z) = -\vec{d}_x \cdot \vec{E}_z(\vec{r}_{//}=0,z) = -ez_0\frac{\Delta\phi_0}{l} \qquad (3.2)$$

The task is to reduce the value of the ratio of the two components of the electric field, in-plane and perpendicular, which behaviour can be seen in Fig. 2.4 and Eq. 2.5, for small values of the normal position of the DQW plane, $z/l$. This task was addressed during this internship and the path followed to the design the electrodes through the implementation of the three electrodes design.

## 3.2 Two electrodes design

For the two electrodes design the results have been obtained under the bias $V_{trap} = -10.5V$ and $V_{guard} = -7.5V$. The in-plane component of the electric field represents the limitation of this simple design. The perpendicular component of the field represents the region in which the excitons are confined, following the knowledge of paragraph 2.3.

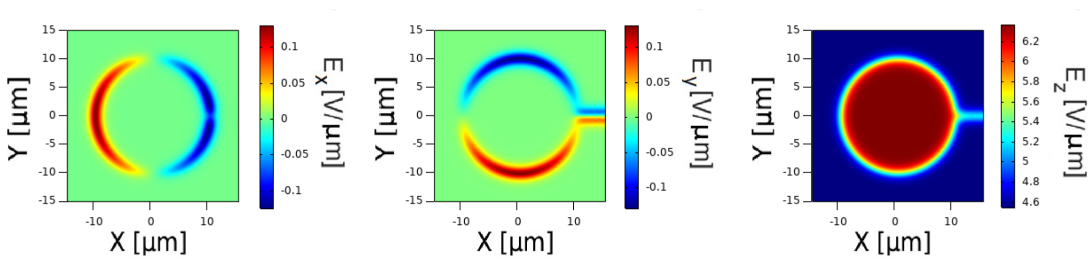


**Figure 3.3:** Simplest design electric field components in the plane of double quantum wells.

In Fig. 3.4 a quantitative insight on the components $E_x$, $E_y$ and $E_z$ of the electric field is observed. Exploiting the symmetry of the system, the electric field is represented along two perpendicular cuts in the plane of the double quantum wells. The results of the perpendicular component of the electric field allow the evaluation of the confinement energy through the Eq. 2.3 which value is in the order of magnitude of meV.

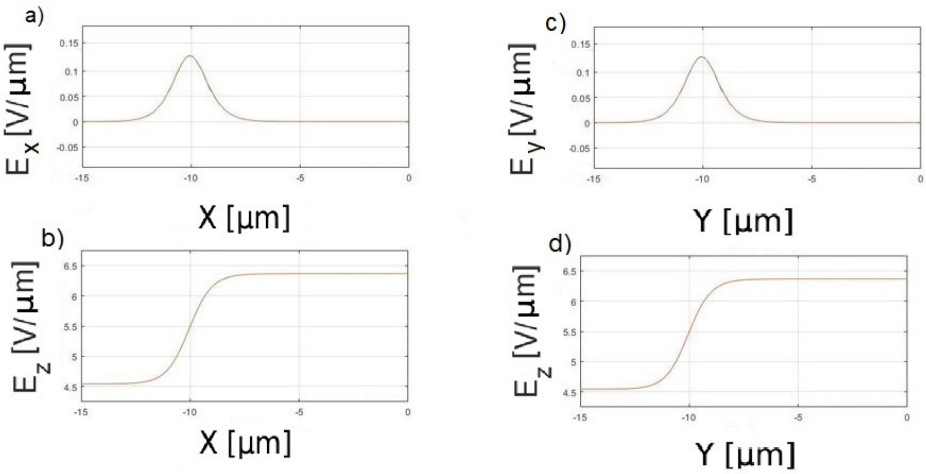


**Figure 3.4:** Electric field components in the plane of the DQW,$E_x$ and $E_y$ and perpendicular to the DQW plane, $E_z$ along the x direction (a-b) and y direction (c-d)

In the previous graphs the symmetry of the system have been exploited in order to represent only the non repetitive parts of the system. To get the idea of the confinement all the device is taken into account, as shown in Fig. 3.5

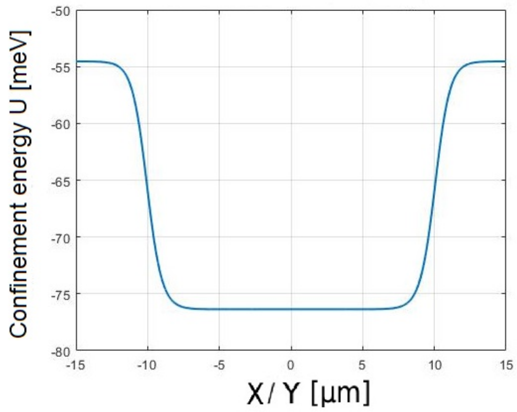


**Figure 3.5:** Confinement energy across is shown the whole device for the circular design in order to emphasize the box-like shape of the confinement

## 3.3 Three electrodes design

In order to bias separately the trapping region, the wire and the guarding region, the three electrodes design was implemented. This more advanced trap design offers great promises to study exciton quantum gases in a model environment, free from excess charges.


**Figure 3.6:** a) The flat trap bias set is represented: the trap (inner blue region) and the guard (external blue region) are both biased at the same voltage therefore represented with the same color. The wire is bias at a different voltage. b) The guard, the wire and the trap in the non-flat trap are biased each at a different voltage. The bias set for the non-flat trap is specified in Fig. 3.7

### The flat trap

The initial proposed method to solve the problem of the high in-plane electric field component was to insert a wire along the border of the trapping region, and in this region then apply the bias voltage of the guard of the simple design.
In this design the wire acts like a barrier, the same voltage is applied to the trap and the guard electrodes. Nevertheless the parametric study that has been carried out on the possible values of the guard's width, none of the value simulated showed a better behaviour for the in-plane component of the electric field and furthermore a worst confining energy was obtained.

### The non-flat trap

The successive step was to bias separately the wire surrounding the trap region and the external region, leading to the non-flat trap for the three electrodes design. The results for the electric field are shown in Fig. 3.7. In order to bias properly the three different regions of the three electrodes design a slight asymmetry is present in the in-plane component of the electric field.

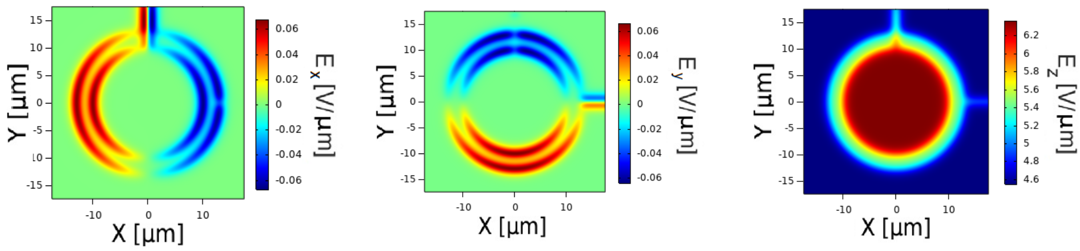


**Figure 3.7:** In-plane component and perpendicular component of the electric field in the three electrodes design under the bias set $V_{trap} = -10.5V$, $V_{wire} = -9.0V$ and $V_{guard} = -7.5V$. This results were obtained with the simulations with a wire's width of 2.75 $\mu$m.

### 3.3.1 Non-flat trap wire's width study

Different values for the wire's width were simulated. The system has two limits on its behaviour depending on the wire.

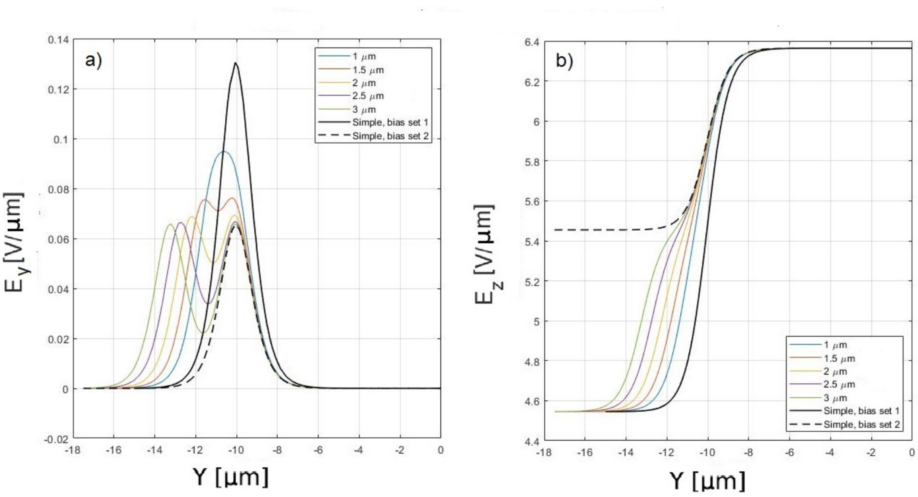


**Figure 3.8:** Results of the in-plane electric field and perpendicular component for the parametric sweep pf the wire from 1 $\mu$m up to 3 $\mu$m. The comparison with the simple trap is possible through two different bias sets, in which the $V_{trap} = -10.5V$ and $V_{guard} = 9V$ and $V_{guard} = -7.5V$ is used as other applied voltage

First, when the wire is thick the electric field behave like the simple design in which the bias applied to the wire has the role of the guard in the simple design. What is most important is that being the wire being biased at an lower value than the

guard bias in the first simple design the barrier height is reduced. Therefore this limit should be avoided.
Second, when the wire's width is decreased under a limit value the in-plane electric field reaches high values. This limit should be avoided, this leaves a possible interval of values to study. The aim of this internship is to study this interval of possible values.
The results of the simulations for the in-plane and perpendicular component of the electric field for this range of values for the guard's width are represented in Fig. 3.8. The reduction for the in-plane electric field is observed in the interesting range of values for the wire's width before its behaviour start to be correlated to a bending in the perpendicular component of the electric field.

## 3.4 Conclusion

In conclusion the analysis that has been carried out with the aim of reducing the in-plane electric field in the excitons confining devices was proven to be successful. The two-fold reduction of the in-plane electric field was achieved through the design of three electrodes design. The three electrodes design was then investigated under the parametric sweep of the value of the guard's width for a set of value which were considered to be interesting based on the knowledge of the behaviour of the system.

### 3.4.1 The electric field components

In the left most graph, Fig.3.9(a), the amplitude of the perpendicular component of the three electrodes design is compared with the the simple design component. In the right graph, Fig.3.9(b), the amplitude of the in-plane component is compared with the simple design component. The interested interval of values for the wire's width happens when the reduction of the in plane electric field component is observed while the perpendicular component remains fixed. The correlated variable for the aimed reduction of the in-plane component of the electric field is the perpendicular component of the electric field. The perpendicular component of the electric field is the key to achieve the confinement and the difference in the energy in the regions in which a bias is applied represents the confinement energy.
For a three electrodes design the aim to have a confinement energy not less than the simple design and that the voltage applied to the wire won't influence the behaviour of the energy i.e. creating distortion. As seen in Fig. 3.9 the two-fold reduction of the in-plane electric field was observed in the simulations alongside the avoided distortion for the perpendicular component of the electric field.

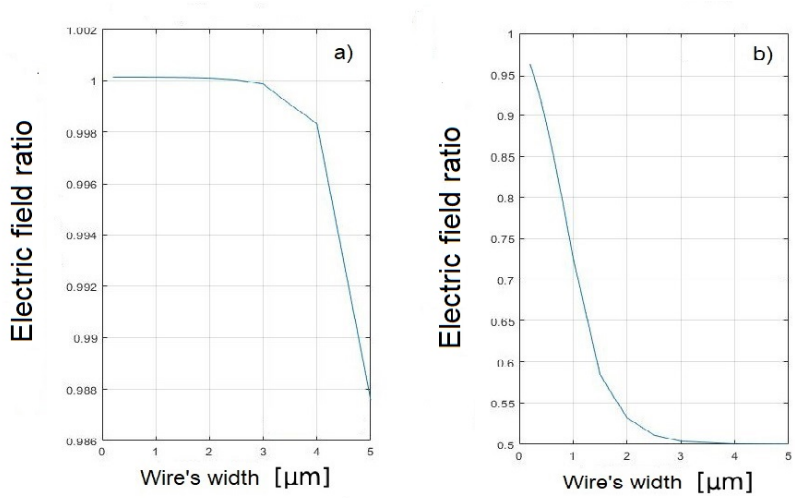


**Figure 3.9:** a) The ratio of the amplitudes of the perpendicular component of the electric field shows a plateaux of value one almost up to 3 $\mu$m and then it drops of few percents. b) The ratio of the amplitudes of the in-plane component of the electric field shows a drop that reaches the two-fold reduction in the interval [1.5 $\mu$m, 2.5 $\mu$m] and then it settles for higher values of the wire's width.

### 3.4.2 Values for the wire's width

The range of values for the guard's width within the two-fold reduction of the in-plane electric field component and the unchanged behaviour for the perpendicular electric field component is from 1.5$\mu$m to 2.5$\mu$m. This was one of the main results of this internship, this study on three electrodes design cleared a possible path of implementation for new devices with improved behaviour with respect to the the simple design, allowing the study of super-fluids of excitons with large spatial extension in an ideal environment.

# Chapter 4

# Two dimensional lattices

In this chapter, we emphasise lattice trapping potentials for dipolar excitons. At first, we introduce the state of the art design of T = 3 µm from [7]: a first electrode imprinting the region of the trap, which is biased stronger than the second electrode defining the electrostatic potential in the guard region. We show that design is the state of the art, but nevertheless limited by behaviour of the electric-field in the plane of the double GaAs quantum wells. The mismatch of along the two directions in the plane of the double quantum well for the electric field is an addressed issue that we solve by working on the geometry of the interdigitated electrodes of the lattice.
We then discuss a more advanced design that allows one to partially circumvent the limitations in the implemented physics of the T = 3 µm lattice design. This more advanced architecture was developed during this internship. It relies on a lattice of period T = 1.5 µm, in order to have a better sample to study the physics of indirect excitons in lattice. Thus, we show that we essentially reduce the lattice period around two-fold, showing that represent an effective device implementation beyond the initial state of the art lattice.

## 4.1 Interdigitated electrodes

Lattice potentials with energy modulation in one dimension were created for indirect excitons by interdigitated gates as shown in Fig. 4.1. A two-dimensional (2D) lattice for excitons can be generated by a two electrodes. The lateral modulation of the perpendicular component of the electric field, which determines the lattice depth, can be controlled by changing the voltage applied to the electrode. The lattice constant and lattice structure are determined by the electrode pattern.

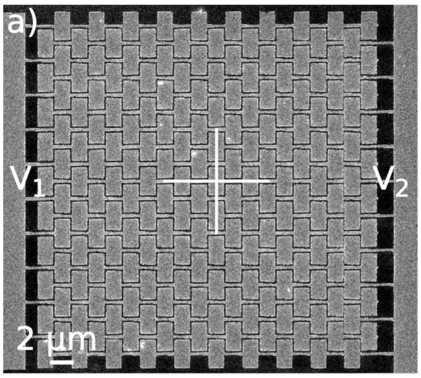


**Figure 4.1:** The image of the two dimensional lattice is obtained through the scanning electron microscope. The two interdigitated electrodes are observed for the T = 3 µm period. Two voltages are applied $V_1$ and $V_2$ in order to define the trapping regions and guarding regions for the study of indirect excitons.

# 4.2 The 3 µm period lattice

## 4.2.1 Design symmetric electric field

As a part of this internship's aim the objective was to work on the state of the art results on previous lattice design as shown in Fig. 4.2(a). In order to do so it was necessary first to study the previous state of the art to improve it.

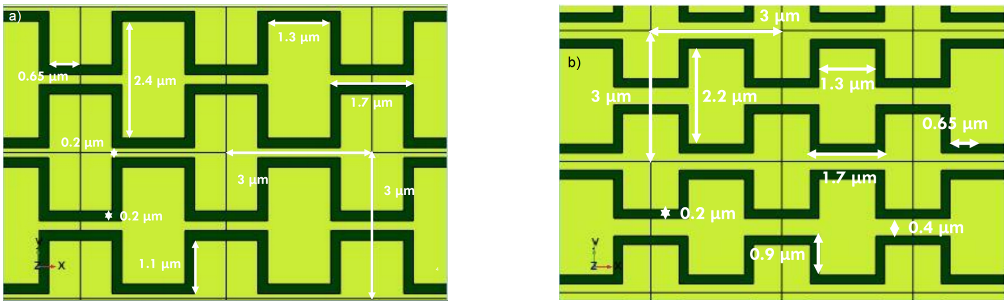


**Figure 4.2:** a) The previous state of the art design for the 3 µm period is presented with all the geometrical characteristic. b) The new designed geometry for the square lattice with the new numerical values of the characteristic.

The in-plane component and the perpendicular component of the electric field were studied. During the study of lattices it was no longer possible to exploit *a priori* a symmetric behaviour in the results of the simulation along the two orthogonal dimensions of the double quantum well plane like the circular design.

### Addressed issues

For the previous state of the art square lattice design a flaw was present: the steepness of the perpendicular component of the electric field was different along the two orthogonal directions of the double quantum well plane and neither the amplitude of the in-plane component of the electric field was matching along the same directions as shown in Fig. 4.3.
Therefore the confinement energy was not equal alongside the previous mentioned axis, being its evaluation the Eq. 2.3. The work that has been carried out was though to modify the geometry of the top contacts of the two dimensional lattice to try to match every component of the electric field, namely the in-plane component and the perpendicular component such that also the confinement energy would match, along the perpendicular directions in the double quantum well plane.

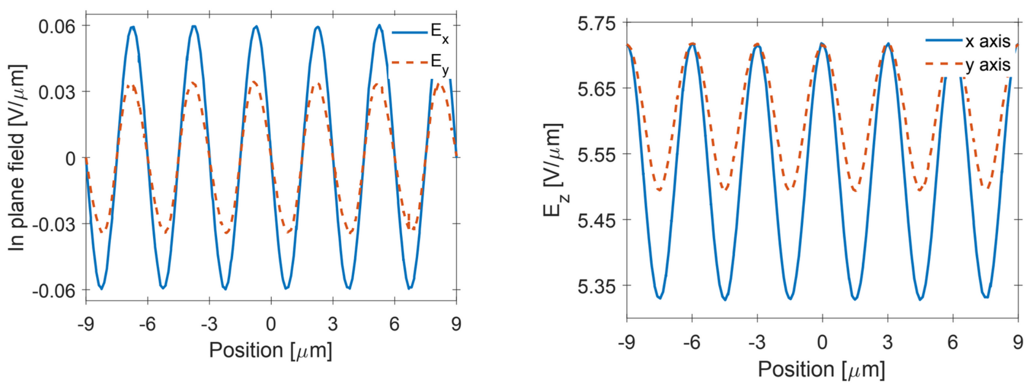


**Figure 4.3:** The first design of the T = 3 $\mu$m was characterized by the side of the rectangular pads with value 2.4 $\mu$m.

## 4.3 Reducing lattice spatial period

Lattices are meant to study phase transitions in which the physics is controlled through the balance of tunneling between neighbouring sites and on-site interactions, directly connected with the requirement of small period values. The optimization of the shape of the lattices is fundamental: this translates into a work on the lattice period. The lattice period should be reduced to the lowest value possible achievable with the current technological processes.
The starting value for the period of square lattice was the already state of the art value of T = 3 µm m and the aim of this internship is to go beyond such value.

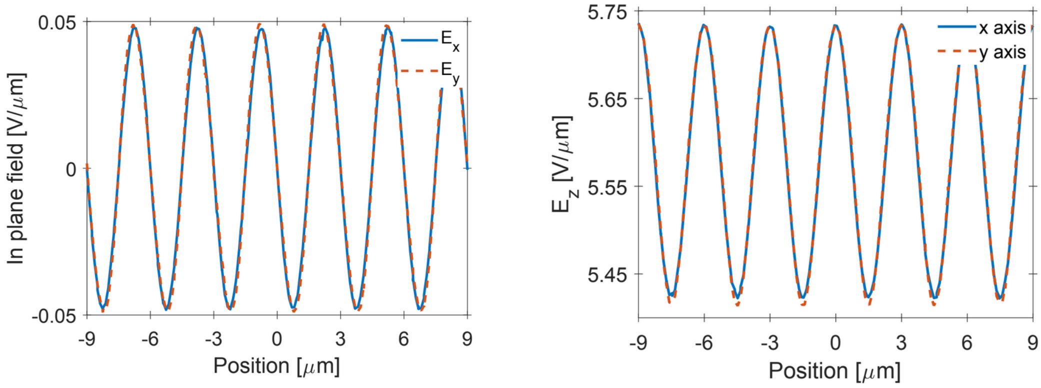


**Figure 4.4:** The second design of the T = 3 $\mu$m was characterized by the side of the rectangular pads with value 2.2 $\mu$m. The matching condition was achieved for the components of the electric field in the plane of the double quantum wells.

Another reason behind the reduction of the lattice period is the aimed result of reducing the number of indirect excitons per site of the lattice because a lower number of particles per site would increase the effectiveness of the confinement.

### 4.3.1 Limitation in downscaling

#### Confinement energy limit and substrate thickness

The strong dipolar repulsive interaction between indirect excitons directly implies that the amplitude of the confinement energy should be greater than a threshold value. The interaction energy of indirect excitons is in the order of magnitude of 1 meV. The threshold value is set up is set up to be 2 meV as an important bench march for the different simulated lattices, as shown in Fig 4.5.

#### Device limits

The limits in the processing of the samples are currently given by the technological process implemented. The electron beam lithography used to process the sample to patter the top electrodes of the square lattices limits the possibility of down scaling. The spacing between the pads of the squared lattice can't go under the value of 150 nm. This constraints and loss of degree of freedoms for the possible geometries of the pads imposes severe limits in the design of the device.

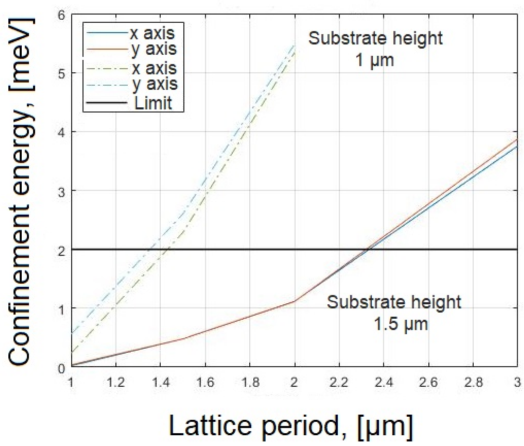


**Figure 4.5:** In order to satisfy the threshold imposed by the interaction energy of indirect excitons, different values for the period of the square lattice were simulated. The difference between the continuous lines (blue and orange) and the dotted lines (green and light blue) is the height of the substrate. For the first one the substrate is 1.5 μm while for the second ones is 1 μm. Due to this difference the T = 2 μm period changes from having an amplitude of the confinement energy below the limit value to above the threshold.

## 4.4 Two-fold period reduction - 1.5 μm lattice

The actual design is shown in Fig. 4.6. In order to study the Bose Hubbard model for indirect excitons it is possible to operate on the parameters $J$ and $U$ by means of the design of the lattice. The results of the two-fold reduction of the period are an increased tunnel between lattice sites and a reduction of the number of excitons per sites up to a four fold reduction of the number. The number of excitons is decreased by an order of magnitude from hundreds to tens of indirect excitons per site.

### 4.4.1 Results

The results for the in-plane component and perpendicular component of the electric field for the T = 1.5 μm show a mismatch in the amplitude along the two directions of the quantum well plane . Nevertheless this mismatch is in the order of few percent for this preparatory work on this new design for the lattice period therefore it actually constitute a valid starting point for an experimental implementation. In order to fulfill the request on the confinement energy as shown in Fig. 4.5 the simulations for this sample were done with a substrate value of 1 μm.

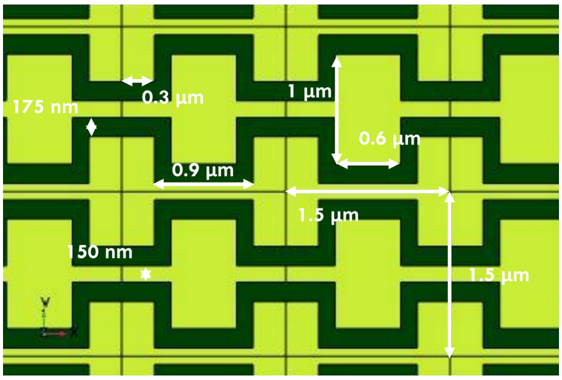


**Figure 4.6:** The core work of the internship was to find the right geometric proportion for the two-folded period lattice considering the present limitations.

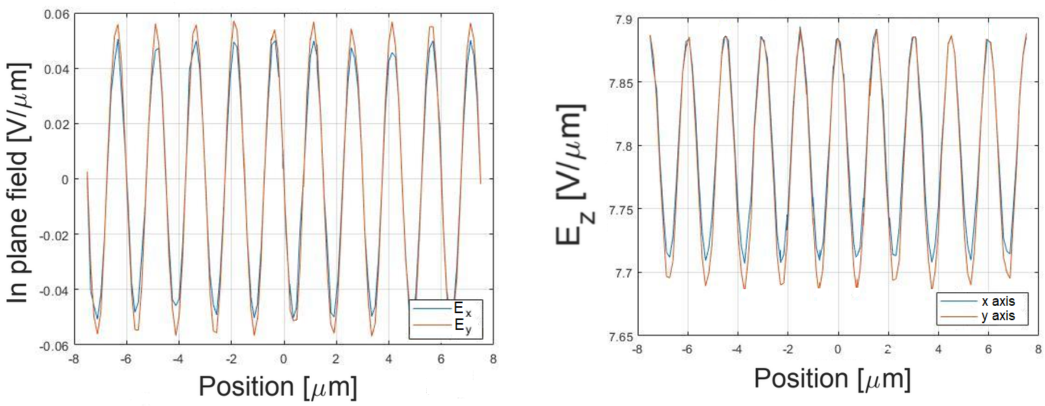


**Figure 4.7:** Perpendicular and in-plane components of the electric field in the T = 1.5 µm design under with substrate of 1 µm the bias set $V_{trap}$ = -10.5 V and $V_{guard}$ = -7.5 V in the double quantum well plane

## 4.4.2 Comparison of the 3 µm lattice and 1.5 µm

Extracting important physical values out of the simulations allows to fully envelop the work that has been carried out. In table 4.1 by comparing the confinement energy $U_x$ and $U_y$ and the ratio of the in-plane component and the perpendicular component of the electric field for the improved T = 3 µm design and T = 1.5 µm.

| Lattice period | Confinement energy | Electric field ratio $E_r/E_z$ |
|---|---|---|
| T = 3 µm (Fig.4.2-b) | $U_x = U_y \sim 3$ meV | 0.385 |
| T = 1.5 µm | $U_x \sim 2.1$ meV, $U_y \sim 2.4$ meV | $E_x/E_z \sim E_y/E_z \sim 0.4$ |

**Table 4.1:** It's possible to observe how the confinement energy never falls below the threshold value and how the ratio of the electric field components it's not drastically increased

## 4.5 Conclusion

In conclusion the two-fold reduction of the lattice period for the square lattice was actually demonstrated to be a possible implementation for the study of indirect excitons. The design and the simulation of the geometry for the square lattice was done through the tools of Comsol Multiphysics.
The study of the electric field in the plane of the double quantum well for the T = 1.5 µm lattice fulfill the wanted limit for the in-plane component of the electric field and the confinement energy threshold for the indirect excitons due to their dipolar nature. Nevertheless in order to achieve such conditions a thinner substrate had to be implemented: the two-fold reduction of the period of the lattice required a smaller value for the substrate height in order to be an actual device, as shown in the road map in Fig. 4.5.

### 4.5.1 Implemented physics

The road map of the reduction of the period of the lattice is implemented in order to explore the Bose Hubbard model in the regime where tunnelling can compete with on site interactions. The work of this internship represents the first step toward this direction, nevertheless it is required to go forward.
It is required to really go to less than microns in terms of the lattice period to exploit the quantum nature of the physics of indirect excitons. In order to achieve results for even smaller period for the lattice it is necessary as consequence to work on even thinner substrate, reducing its value from the already reduced value of 1 µm implemented for the new two-fold reduced lattice period of 1.5 µm lattice period.

# Bibliography

[1] M. H. Anderson, J. R. Ensher, M. R. Matthews, C. E. Wieman, and E. A. Cornell. «Observation of Bose-Einstein Condensation in a Dilute Atomic Vapor». In: *Science* 269.5221 (1995), pp. 198–201. ISSN: 00368075, 10959203. URL: `http://www.jstor.org/stable/2888436` (cit. on pp. 1, 2).

[2] Makoto Tsubota and Kenichi Kasamatsu. «Quantized vortices in superfluid helium and atomic Bose-Einstein condensates». In: (Apr. 2010). DOI: `10.1093/acprof:oso/9780199585915.003.0003` (cit. on p. 1).

[3] Elliott E.R. et al. Aveline D.C. Williams J.R. «Observation of Bose–Einstein condensates in an Earth-orbiting research lab». In: *Nature* 582 (June 2020), pp. 193–197. DOI: `10.1038/s41586-020-2346-1` (cit. on p. 1).

[4] Markus Greiner, Olaf Mandel, Tilman Esslinger, Theodor Haensch, and Immanuel Bloch. «Quantum phase transition from a superfluid to a Mott insulator in a gas of ultracold atoms». In: *Nature* 415 (Feb. 2002), pp. 39–44. DOI: `10.1038/415039a` (cit. on p. 2).

[5] C. Salomon, G Shlyapnikov, and Leticia Cugliandolo. *Many-Body Physics with Ultracold Gases: Lecture Notes of the Les Houches Summer School: Volume 94, July 2010*. Jan. 2012. DOI: `10.1093/acprof:oso/9780199661886.001.0001` (cit. on p. 3).

[6] Monique Combescot, Roland Combescot, and François Dubin. «Bose–Einstein condensation and indirect excitons: a review». In: *Reports on Progress in Physics* 80.6 (Mar. 2017), p. 066501. DOI: `10.1088/1361-6633/aa50e3` (cit. on pp. 4, 6, 7).

[7] Mikas Remeika, Michael Fogler, L.V. Butov, Maxwell Hanson, and A.C. Gossard. «Two-Dimensional Electrostatic Lattices for Indirect Excitons». In: *Applied Physics Letters* 100 (Feb. 2012), pp. 061103–061103. DOI: `10.1063/1.3682302` (cit. on pp. 4, 22).

[8] Gang Chen, Ronen Rapaport, L. Pffeifer, Kayte West, P. Platzman, Steven Simon, Z. Voros, and David Snoke. «Artificial trapping of a stable high-density dipolar exciton fluid». In: *Physical Review B* 74 (Jan. 2006). DOI: 10.1103/PhysRevB.74.045309 (cit. on p. 9).

[9] A. Honold, L. Schultheis, J. Kuhl, and C. W. Tu. «Collision broadening of two-dimensional excitons in a GaAs single quantum well». In: *Phys. Rev. B* 40 (9 Sept. 1989), pp. 6442–6445. DOI: 10.1103/PhysRevB.40.6442. URL: https://link.aps.org/doi/10.1103/PhysRevB.40.6442 (cit. on p. 10).

[10] Romain Anankine, Suzanne Dang, Mussie Beian, Edmond Cambril, Carmen Gomez Carbonell, Aristide Lemaître, and François Dubin. «Temporal coherence of spatially indirect excitons across Bose-Einstein condensation: The role of free carriers». In: *New Journal of Physics* 20 (July 2018), p. 073049. DOI: 10.1088/1367-2630/aad30a (cit. on p. 10).

[11] Ronen Rapaport, Gang Chen, Steven Simon, Oleg Mitrofanov, Loren Pfeiffer, and P. M. Platzman. «Electrostatic traps for dipolar excitons». In: *Phys. Rev. B* 72 (7 Aug. 2005), p. 075428. DOI: 10.1103/PhysRevB.72.075428. URL: https://link.aps.org/doi/10.1103/PhysRevB.72.075428 (cit. on p. 11).